DELFT UNIVERSITY OF TECHNOLOGY

REPORT 16-07

A network model for the biofilm growth evolution in porous media and its effects on permeability and porosity

L.A. Lopez Peña, B. Meulenbroek and F.J. Vermolen

ISSN 1389-6520

Reports of the Delft Institute of Applied Mathematics

Delft 2016

A network model for the biofilm growth evolution in porous media and its effects on permeability and porosity

Luis A. Lopez-Peña [1], Bernard Meulenbroek [1], and Fred Vermolen [1]

[1] *Delft Institute of Applied Mathematics, Delft University of Technology, Mekelweg 4, 2628 CD, Delft, The Netherlands*

The success of the application of Microbial Enhanced Oil Recovery (MEOR) techniques depends on several factors such as individual reservoir characteristics and microbial activity. Since the quantification of the relations between the aforementioned parameters is difficult to obtain, the development of mathematical and numerical models predicting the bacterial population growth and in situ production of by-products is of vital importance to develop a proper field strategy [15]. In this work, we use a pore network model to study the hydrodynamic changes over time on a porous medium as a result of biofilm growth. We propose a new model in the microscopic scale for biofilm growth which allows the spreading of the biofilm over the network. This formalism for the biofilm growth leads to a new relation between the permeability and the amount of biomass in the network. These results could be up-scaled to the continuum-based oil reservoir scales.

1 Introduction

Oil recovery is typically divided into three stages. In primary extraction, the oil production from the wells is the result of the natural pressure of the oil. When the primary production declines some wells are converted into injection wells and waterflooding or gas flooding techniques are implemented to extract oil during the secondary recovery. After primary and second recovery two-thirds of the oil remain trapped in the ground [4]. Therefore, some techniques have been developed to extract the remaining oil trapped in the reservoir. Among these techniques, there are methods such as polymer flooding and surfactant flooding which are chemical oil recovery methods and microbial enhanced oil recovery (MEOR) techniques. In MEOR techniques, the growth of bacteria and the resulting by-products are used in order to increase residual oil production. Microbial growth may enhance oil displacement by increasing the efficiency of waterflooding process, interfacial tension reduction and rock wettability change [1,9]. It seems to be that interfacial tension

reduction and the increase of water flooding efficiency caused by selective plugging are the mechanisms that have the most impact on oil recovery.

During microbial growth, bacteria adhere to the walls of the pores within a self-produced matrix of extra cellular polymeric substances (EPS). The adhered bacteria and the self-produced matrix are usually referred to as biofilm. Microbial growth has a direct impact on hydraulic properties of the porous media. The accumulation of bacteria biomass can lead to the reduction of the permeability and porosity due to the plugging of the pores by the biomass [17]. The relation between permeability and porosity is usually described by the Kozeny-Carman relation. Even though this model is widely accepted it has some limitations [21]. In order to improve the accuracy of the estimation of the permeability, many semi empirical corrections to the Kozeny Carman equation have been proposed, see for instance Costa et al. [6].

The aim in selective plugging is that biofilm grows preferentially in the high permeability zones, causing the diversion of the water-flood from the thief zones towards oil-rich areas. Typically in MEOR techniques, indigenous bacteria population growth is supported by the injection of nutrients into the reservoir [15].

In laboratory experiments and in field trials an increase of oil production due to MEOR techniques has been reported [3,10,22]. However, the experimental study is complex due to the different parameters involved and the slow rates of biofilm growth [14]. Therefore, the development of mathematical and numerical models predicting the bacterial population growth, nutrients transport, in situ production of by-products and the permeability and porosity changes due to biofilm growth are of vital importance to develop a proper field strategy [15].

The influence of biofilm growth on permeability has been modeled using a mathematical description based on a theoretical framework and phenomenological relations resulting from experimental results [14, 17]. Among mathematical models developed to describe biofilm growth on porous media, there exist continuum Darcy models [20], bacterially-based models [11], Lattice Boltzmann based simulations [8, 12] and Pore Network Models (PNM) [5,7,16,19]. Usually, in biofilm growth models the porous medium consists of three components: the grains, the biofilm which grows on the walls of the solid grains and the liquid in the pore space. The grains are assumed to be impermeable to the liquid and the nutrients, therefore hydrodynamic model equations are written only for the liquid and biofilm [12].

In PNMs, the porous medium is considered as cylindrically interconnected tubes in which the water can flow. The temporal evolution of the process is described by transport of nutrients through the network, bacterial population growth and biofilm development. Transport of nutrients is carried out within an aqueous phase and is described by a convection diffusion equation with a reaction term that models the consumption of nutrients caused by bacterial population growth. The bacterial population will determine the development of biofilm in the pores of the medium. This biofilm will grow and will change the radii of the pores, leading to a modification in the dynamics of the fluid that carries the nutrients through the network [5, 7, 16, 19].

The Monod equation is often used to describe the growth of bacteria in the pores [5, 7,

..	..	..	..	$n_{N_x \times N_y}$
..	..	..	..	..
..	..	n_{i+N_x}	..	..
..	n_{i-1}	n_i	n_{i+1}	..
..	..	n_{i-N_x}	..	..
n_{Nx+1}	..	..	..	..
n_1	n_2	..	..	n_{Nx}

Table 1: Order of the nodes in the network

16, 18]; this equation relates the growth rate of bacteria to the concentration of nutrients available in the network.

In this study, we model the biomass growth and the transport of nutrients in a porous medium using a pore network model to represent the porous medium. We consider the biofilm as an impermeable layer which is able to grow when it come into contact with the nutrients. We present a new model in which the biofilm growth depends on the interfacial area between biofilm and water. This assumption allows the spreading of biofilm through the whole network. This formalism for the biofilm growth leads to a new relation between the permeability and the amount of biomass in the network which can be effectively described by an explicit equation.

This paper is organized as follows: in Section 2, we describe the physical, mathematical and biological considerations that are involved in the process of bioclogging in a porous medium. We illustrate how we model the porous medium, the injection of nutrients, and the growth and development of biofilm. In Section 3, the numerical method used is described and the computational steps are explained. In Section 4 the results are presented. Finally, in Section 5 the discussion and the conclusions are drawn and the outlook to other problems is presented.

2 Mathematical model

We represent the porous medium as a 2D network composed of interconnected cylindrical tubes. The point where these tubes are connected is called a node of the network, and is indexed as node n_i. The tube between the node n_i and n_j is indexed as the tube t_{ij} (see Figure 1). We assume that all the tubes have the same radii (which differs from previous studies because we want to express the spreading of the biofilm in terms of differences of biofilm volume between neighboring tubes in a simple way, see spreading of the biofilm) and the same length l. The number of tubes connected in each node is four for interior nodes, three for boundary nodes and two for the nodes in the corner of the network.

We consider the bacteria and the biofilm lumped together and we refer to them as biofilm. We assume that in 4% of the tubes there is an initial volume of biofilm attached to the walls of the tubes. Initially nutrients are not present in the network, therefore nutrients need to be injected through the network and transported within a fluid.

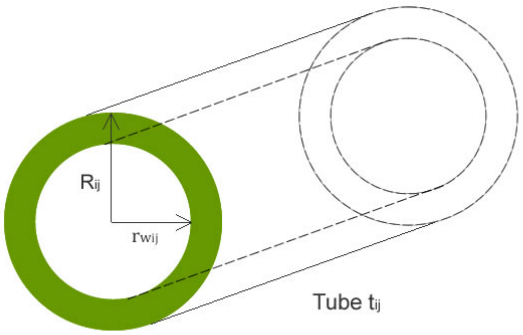

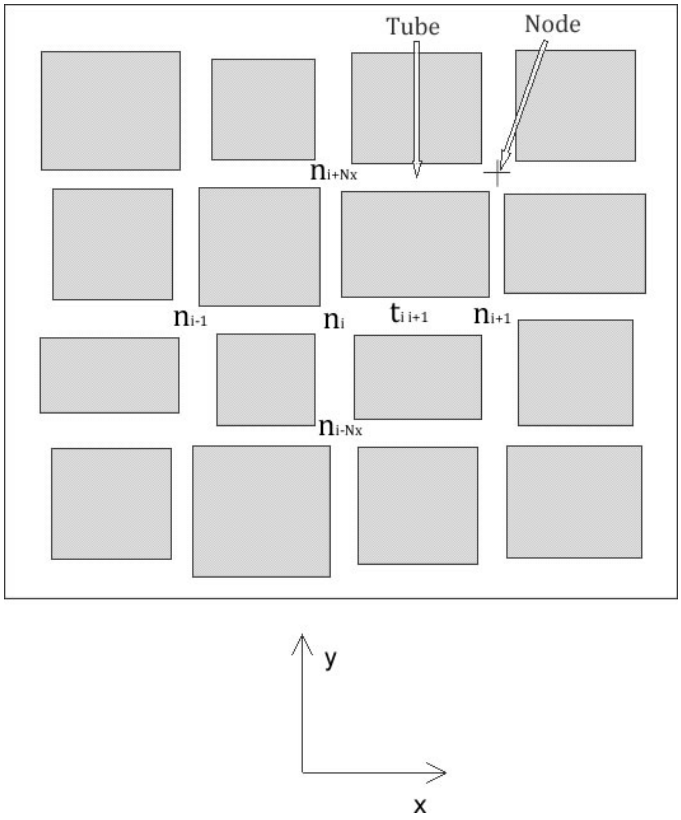

Figure 1: Pore Network and tubes

We define the thickness of the biofilm in the tube t_{ij} as $r_{b_{ij}}$, the radius of tube available for water by $r_{w_{ij}}$ and the total radius of the tube by R_{ij} (see Figure 1).

The volumetric flow of the aqueous phase q_{ij} in the tube t_{ij} is described by a modified form of the Poiseuille equation [18],

$$q_{ij} = \frac{\pi}{8\mu l}[r_{w_{ij}}^4 + (R_{ij}^4 - r_{w_{ij}}^4)\beta^{-1}]\Delta p, \tag{1}$$

where Δp is the pressure drop between these neighboring nodes, μ is the viscosity of water that flows in the bulk, β is the ratio between the viscosity of water flowing through the biofilm and the viscosity of water flowing through the bulk and l is the length of the tube. We use $\beta = 10^7$ which according to [18] is a good approximation for an impermeable biofilm.

Mass conservation is imposed in each of the nodes. For the node n_i we have

$$\sum_{j \in S_i} q_{ij} = 0, \tag{2}$$

where $S_i = \{j \mid n_j \text{ is adjacent to the node } n_i\}$ and further q_{ij} is the flux in the tubes connected to node n_i. This mass conservation is analogous to Kirchhoff's current law in electronics.

The transport of nutrients is described by an advection diffusion reaction equation. We denote the concentration of nutrients as C,

$$\frac{\partial C}{\partial t} = -\mathbf{u} \cdot \nabla C + D\nabla^2 C - \frac{\lambda_b^+}{Y}\frac{C}{E_{bs} + C}b, \tag{3}$$

where b is the biofilm concentration (mass per volume), λ_b^+ is a microbial specific growth rate, Y is the yield coefficient, E_s is a saturation constant, D is the diffusion coefficient, and $\mathbf{u}$ is the velocity which is related to the local flux $\mathbf{q}$ by $\mathbf{u} = \mathbf{q}/A$, where A is the area of the cross section of the tube.

We denote the biofilm concentration by b. The concentration b of the biofilm is related to the volume of biofilm by,

$$V_{bf_{ij}} = \frac{b_{ij}}{\rho_{bf}} V_{ij}, \tag{4}$$

where V_{ij} is the total volume of the tube t_{ij}, b_{ij} is the biofilm concentration in the tube t_{ij} and ρ_{bf} is the density of the biofilm, which we assume constant.

In this model we consider the biofilm as an impermeable layer in which nutrients are not able to travel. Hence, the nutrients needed for the biofilm growth, come in contact with the biofilm only at the interface between water and the biofilm. For this reason, we propose that the growth of the volume of biofilm is proportional to the interface area between water and biofilm, A_{wbf}. Furthermore, we assume that the growth of the volume of the biofilm is determined by the concentration of nutrients using the Monod Kinetics equation. There are two mechanisms in which biofilm can grow: as a result of the interior

interfacial water biofilm area or due to the interfacial water biofilm area in the extremes of the tube.

The volume of biofilm that grows in the interior of the tube t_{ij} , $V^i_{bf_{ij}}$ is proportional to the interfacial water biofilm area in the interior A^i_{wbf} of the tube and the concentration of nutrients C_{ij} via Monod Kinetics within the tube t_{ij}, then the biofilm growth in the interior can be written as,

$$\frac{\partial V^i_{bf_{ij}}}{\partial t} = k_1 \frac{A^i_{wbf}}{A^i_T} V_T \frac{C_{ij}}{E_s + Cij}, \tag{5}$$

in in this equation, k_1 is a growth rate constant, A_T is the external area of the tube and V_T is the total volume of the tube. The ratio between the interior interfacial water biofilm area A^i_{wbf} and the total area of the tube A^i_T is a measure of the biofilm growth within the tube. This ratio is zero when there is no biofilm in the tube or when the tube is filled with biofilm, consequently, biofilm growth in the interior of the tube stops when there is no more space in the tube. Further, the area A^i_{wbf} can be written in terms of the total volume of the pore V_{ij} and the volume of biofilm V_{bf}, therefore the equation for the biofilm which grows in the interior, $V_{bf_{ij}}$, is

$$\frac{\partial V^i_{bf_{ij}}}{\partial t} = k_1 R \frac{C_{ij}}{E_s + Cij} \sqrt{\pi l (V_{ij} - V_{bf_{ij}})}, \text{ if } V_{bf_{ij}} > 0 \tag{6}$$

in which R is the radius of the tube. If there is no initial biofilm in the tube, the interfacial water biofilm area is zero, therefore there is no biofilm growth in the interior of the tube,

$$\frac{\partial V^i_{bf_{ij}}}{\partial t} = 0, \text{ if } V_{bf_{ij}} = 0. \tag{7}$$

The biofilm growth in the extremes of the tube depends on the interfacial water biofilm area between neighboring tubes. We consider binary interaction with the neighboring tubes. Since all the radii of the tubes are the same, the area A^e_{wbf} between the tube t_{ij} and the tube t_{jk} can be written in terms of the volume of the biofilm of neighboring tubes. Therefore, if the volume of biofilm $V_{bf_{jk}}$ in the neighboring tube t_{jk} (connected to the node n_j) is larger than the volume of biofilm $V_{bf_{ij}}$ in the tube t_{ij}, then biofilm will be produced in the extreme of the tube t_{jk} and it will be given to the tube t_{ij}. Further, no biofilm will be produced in the extreme close to the node j of the tube t_{ij} (see figure 3). On the other hand, if the volume of biofilm $V_{bf_{jk}}$ in the neighboring tube t_{jk} (connected to the node n_j) is less than the volume of biofilm $V_{bf_{ij}}$, the biofilm will be produced in the extreme of the tube t_{ij} and it will be given to the neighboring tube t_{jk}.

If we assume that the volume of biofilm $V_{bf_{jk}}$ in the neighboring tube t_{jk} (connected to the node n_j) is larger than the volume of biofilm $V_{bf_{ij}}$ in the tube t_{ij}, then the biofilm growth in the extreme of the neighboring tube t_{jk} will be proportional to the water biofilm interface area in the extreme A^e_{wbf}. Furthermore, this biofilm growth depends on the concentration of nutrients within the tube t_{jk} via Monod Kinetics,

$$\frac{\partial V^e_{bf_{jk}}}{\partial t} = k_1 \frac{A^e_{wbf}}{A^e_T} V_T \frac{C_{jk}}{E_s + C_{jk}}, \tag{8}$$

in which A^e_T is the cross-sectional area in the extreme of the tube and V_T is the total volume of the tube. The ratio between the external interfacial water biofilm area A^e_{wbf} and the cross-sectional area of the tube A^e_T is a measure of the biofilm growth in the extremes of the tube and then it is a measure of the volume of biofilm interchange between neighboring tubes. This ratio is zero when the volume of biofilm is the same in both interacting tubes which means there is no growth of biofilm in the extreme of the tube and no volume of biofilm will be added to either of them. On the other hand, when this ratio is one, there is no biofilm in the tube t_{ij} and the tube t_{jk} is full of biofilm, then biofilm which grows in the extreme of the tube t_{jk} will grow at maximal rate and the accumulated biofilm will be added to the tube t_{jk}. In this way, this model for the biofilm growth allows the spreading of the biofilm through the whole network, which is consistent with experimental results. The area A^e_{wbf} between the tube t_{ij} and the tube t_{jk} can be written in terms of the volume of the biofilm of the tubes,

$$A^e_{wbf} = \frac{(V_{bf_{jk}} - V_{bf_{ij}})}{l}, \tag{9}$$

hence the equation for the biofilm growth in the extreme of the tube t_{jk} can be written as,

$$\frac{\partial V^e_{bf_{jk}}}{\partial t} = k_1 \frac{C_{jk}}{E_s + C_{jk}} (V_{bf_{jk}} - V_{bf_{ij}}). \tag{10}$$

The tube t_{ij} will receive biofilm from their neighboring tube t_{jk}. To this extent we introduce the following index set notation for the tube t_{ij} which connects nodes n_i and n_j. Consider the node n_j then we define the set of neighboring nodes of it, except n_i by Λ_{ji} (see Figure 1). We take into account all the neighboring tubes whose volume of biofilm are larger than the volume of biofilm in the tube t_{ij}, therefore, the equation for the biofilm growth in the tube t_{ij} due biofilm growth in the extremes of the neighboring tubes is written as,

$$\frac{\partial V^e_{bf_{ij}}}{\partial t} = k_1 \sum_{k \in \Lambda_{ji}} \frac{C_{jk}}{E_s + C_{jk}} (V_{bf_{jk}} - V_{bf_{ij}})_+ + k_1 \sum_{k \in \Lambda_{ij}} \frac{C_{ki}}{E_s + C_{ki}} (V_{bf_{ki}} - V_{bf_{ij}})_+. \tag{11}$$

where the subscript $(V_{bf_{ki}} - V_{bf_{ij}})_+ = max(0, V_{bf_{ki}} - V_{bf_{ij}})$ which means we take into account only the neighboring tubes t_{jk} whose volume of biofilm are larger than the volume of biofilm in the tube t_{ij}.

Finally, when we take into account the interior growth, the biofilm which grows in the neighboring tubes and the detachment of biofilm (which is proportional to the interior interfacial water biofilm area) the equation for the biofilm growth in the tube t_{ij} can be written as,

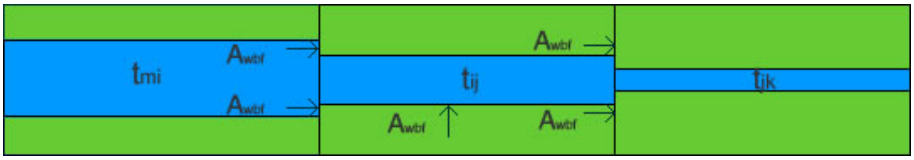

Figure 2: Interfacial water -biofilm area

$$\begin{aligned}\frac{\partial V_{bf_{ij}}}{\partial t} &= k_1 R \frac{C_{ij}}{E_s + C_{ij}} \sqrt{\pi l (V_{ij} - V_{bf_{ij}})} \\ &+ k_1 \sum_{k \in \Lambda_{ji}} \frac{C_{jk}}{E_s + C_{jk}} (V_{bf_{jk}} - V_{bf_{ij}})_+ \\ &+ k_1 \sum_{k \in \Lambda_{ij}} \frac{C_{ki}}{E_s + C_{ki}} (V_{bf_{ki}} - V_{bf_{ij}})_+ - k_2 R \sqrt{\pi l (V_{ij} - V_{bf_{ij}})}, \text{ if } V_{bf_{ij}} > 0\end{aligned} \tag{12}$$

and

$$\begin{aligned}\frac{\partial V_{bf_{ij}}}{\partial t} &= k_1 \sum_{k \in \Lambda_{ji}} \frac{C_{jk}}{E_s + C_{jk}} (V_{bf_{jk}} - V_{bf_{ij}})_+ \\ &+ k_1 \sum_{k \in \Lambda_{ij}} \frac{C_{ki}}{E_s + C_{ki}} (V_{bf_{ki}} - V_{bf_{ij}})_+, \text{ if } V_{bf_{ij}} = 0,\end{aligned} \tag{13}$$

where V_{ij} is the total volume of the pore and C_{ij} is the concentration of nutrients. In equation (12) the first term is the interior biofilm growth, the second and third term describe the biofilm which grows in the extremes of the neighboring tubes and the fourth term is a term for the detachment of the biofilm. When there is no biofilm in the tube equation (13) holds.

The new thickness of the biofilm is computed and it is coupled back to the flux equation (1) and to the conservation mass equation (2).

In summary, the following equations describe the flux within each tube, transport of nutrients within a fluid phase in the network and the biofilm growth in the network,

Poiseuille Flow

$$q_{ij} = \frac{\pi}{8\mu l} [r_{w_{ij}}^4 + (R_{ij}^4 - r_{w_{ij}}^4)\beta^{-1}] \Delta p, \tag{14}$$

Conservation of Mass

$$\sum_{j \in S_i} q_{ij} = 0, \tag{15}$$

Boundary conditions for the resulting system of equations for the pressure,

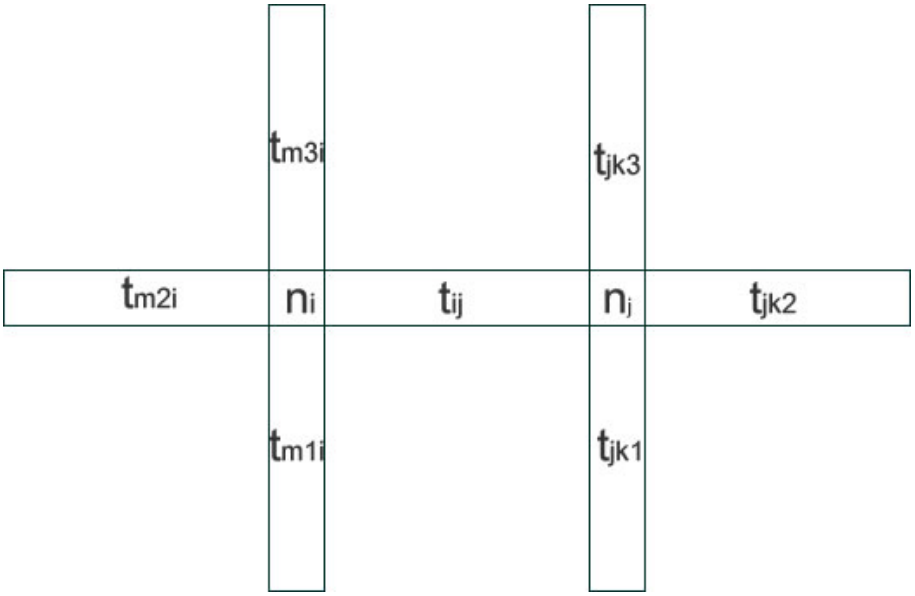

Figure 3: Neighboring tubes

$$\begin{aligned} p(0,y) &= 1600L_x, \\ p(L_x,y) &= 0, \\ \frac{\partial p}{\partial n}(x,0) &= 0, \\ \frac{\partial p}{\partial n}(x,L_y) &= 0, \end{aligned} \tag{16}$$

Transport of nutrients

$$\frac{\partial C}{\partial t} = -\mathbf{u}\cdot\nabla C + D\nabla^2 C - \frac{\lambda_b^+}{Y}\frac{C}{E_{bs}+C}b, \tag{17}$$

Initial condition

$$\begin{aligned} C(x,y,t_0) &= 0, \\ t_0 &= 0, \end{aligned} \tag{18}$$

Boundary condition

$$\begin{aligned} C(0,y,t) &= 1, \\ \frac{\partial C}{\partial x}(L_x,y) &= 0; \end{aligned} \tag{19}$$

Biofilm Growth

$$\frac{\partial V_{bf_{ij}}}{\partial t} = k_1 R \frac{C_{ij}}{E_s + C_{ij}} \sqrt{\pi l (V_{ij} - V_{bf_{ij}})}$$
$$+ k_1 \sum_{k \in \Lambda_{ji}} \frac{C_{jk}}{E_s + C_{jk}} (V_{bf_{jk}} - V_{bf_{ij}})_+ \tag{20}$$
$$+ k_1 \sum_{k \in \Lambda_{ij}} \frac{C_{ki}}{E_s + C_{ki}} (V_{bf_{ki}} - V_{bf_{ij}})_+ - k_2 R \sqrt{\pi l (V_{ij} - V_{bf_{ij}})}, \text{ if } V_{bf_{ij}} > 0.$$

and

$$\frac{\partial V_{bf_{ij}}}{\partial t} = k_1 \sum_{k \in \Lambda_{ji}} \frac{C_{jk}}{E_s + C_{jk}} (V_{bf_{jk}} - V_{bf_{ij}})_+$$
$$+ k_1 \sum_{k \in \Lambda_{ij}} \frac{C_{ki}}{E_s + C_{ki}} (V_{bf_{ki}} - V_{bf_{ij}})_+, \text{ if } V_{bf_{ij}} = 0. \tag{21}$$

For the system of equations resulting from applying mass conservation in each of the nodes $\sum_{j \in S_i} q_{ij} = 0$ we consider Dirichlet boundary conditions for the pressure in the left and right boundaries and no-flux condition in the upper and lower boundaries of the network. Regarding the transport of nutrients, the initial condition for the concentration was set to $C(\mathbf{x}, t) = 0$ in the network. As the injection of nutrients is done in the left boundary, the boundary condition for the concentration was set to one in the left boundary of the network $C(x = 0, y, t) = 1$. Finally, we consider that only 4% of the tubes in the network were seeded initially with a concentration of $b_0 = 10^{-6}$ $[kg/m^3]$.

3 Numerical Method

In this section we are going to outline the numerical procedure used in the model and the computational steps followed in this paper.

Substitution of equation (1) into (2) for each node n_i leads to a linear system for the pressure at the nodes, p_i, as unknowns. This system is solved assuming Dirichlet boundary conditions for the left and right boundary of the network and considering that there is no flow through the upper and lower boundary, therefore $\frac{\partial p}{\partial n} = 0$ is used in this part of the boundary.

After solving the nodal pressures p_i, we can substitute their values into equation (14) to obtain the flux in each tube of the network.

The solution to equation (3) is approximated by the use of the finite differences scheme. Then, for each node the advection diffusion reaction equation can be written as,

$$\frac{\Delta C_i}{\Delta t} = \left[\frac{\Delta C_i}{\Delta t}\right]_{adv} + \left[\frac{\Delta C_i}{\Delta t}\right]_{diff} + \left[\frac{\Delta C_i}{\Delta t}\right]_{reaction}. \tag{22}$$

The advection part can be written as,

$$\left[\frac{\Delta C_i}{\Delta t}\right]_{adv} = \left[\frac{{C_i}^{t+1} - {C_i}^{t}}{\Delta t}\right]_{adv} = \sum_{j\in\Omega_i} \frac{{q_{ij}}^{t}}{V_{ij}}({C_j}^{t+1} - {C_i}^{t+1}), \tag{23}$$

where $\Omega_i = \{j \mid q_{ij} \text{ is directed towards the node } n_i\}$ and V_{ij} is the total volume of the tube.

The diffusion of nutrients is written as,

$$\left[\frac{\Delta C_i}{\Delta t}\right]_{diff} = \left[\frac{{C_i}^{t+1} - {C_i}^{t}}{\Delta t}\right]_{diff} = \frac{D_w}{l^2} \sum_{j\in S_i} ({C_i}^{t+1} - {C_j}^{t+1}) \frac{A^t_{w_{ij}}}{A_{tot_{ij}}}, \tag{24}$$

where D_w is the diffusion coefficient of the water in the free space available for the bulk water. Further, $A_{w_{ij}}$ is the area of the cross section of the bulk water in the tube t_{ij} and $A_{tot_{ij}}$ is the total area of cross section of the tube t_{ij}.

The volume of the biofilm is determined by,

$$\begin{aligned}
\frac{\Delta V_{bf_{ij}}}{\Delta t} &= \left[\frac{{V_{bf_{ij}}}^{t+1} - {V_{bf_{ij}}}^{t}}{\Delta t}\right] = \\
& k_1 R \left[\frac{{C_{ij}}^{t}}{E_{bs} + {C_{ij}}^{t}}\right] \sqrt{\pi l (V_{ij} - V^t_{bf_{ij}})} \\
& + k_1 \sum_{k\in\Lambda_{ji}} \left[\frac{C^t_{jk}}{E_s + C^t_{jk}}\right] (V^t_{bf_{jk}} - V^t_{bf_{ij}})_+ \\
& + k_1 \sum_{m\in\Lambda_{ij}} \left[\frac{C^t_{mi}}{E_s + C^t_{mi}}\right] (V^t_{bf_{mi}} - V^t_{bf_{ij}})_+ \\
& - \ k_2 R \sqrt{\pi l (V_{ij} - V^t_{bf_{ij}})}, \text{ if } V_{bf_{ij}} > 0
\end{aligned} \tag{25}$$

and

$$\begin{aligned}
\frac{\Delta V_{bf_{ij}}}{\Delta t} &= \left[\frac{{V_{bf_{ij}}}^{t+1} - {V_{bf_{ij}}}^{t}}{\Delta t}\right] = \\
& + k_1 \sum_{k\in\Lambda_{ji}} \left[\frac{C^t_{jk}}{E_s + C^t_{jk}}\right] (V^t_{bf_{jk}} - V^t_{bf_{ij}})_+ \\
& + k_1 \sum_{m\in\Lambda_{ij}} \left[\frac{C^t_{mi}}{E_s + C^t_{mi}}\right] (V^t_{bf_{mi}} - V^t_{bf_{ij}})_+, \text{ if } V_{bf} = 0.
\end{aligned} \tag{26}$$

Using equation (4) we can express the volume of biofilm $V_{bf_{ij}}$ as the concentration of biofilm b_{ij} in each tube. However, in order to give an expression for the last term of equation (3) we need to know the concentration of biofilm in each node, b_i, then we average the concentration of biofilm of the tubes connected by the node n_i,

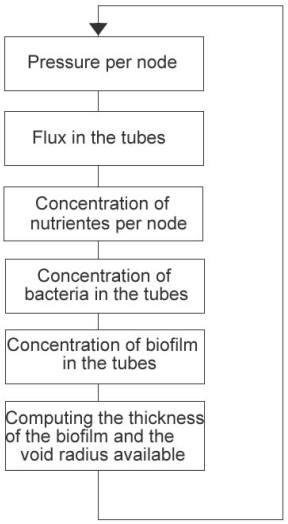

Figure 4: Flow Chart for each time step

$$\frac{\sum_{j\in S} b_{ij}V_{ij}}{\sum_{j\in S} V_{ij}} = b_i. \tag{27}$$

Now the reaction term of equation (3) can be written as,

$$\left[\frac{\Delta C_i}{\Delta t}\right]_{reaction} = \left[\frac{{C_i}^{t+1} - {C_i}^{t}}{\Delta t}\right]_{reaction} = \frac{\lambda_b^+}{Y}\frac{C_i^{t+1}}{E_s + C_i^t} b_i^t. \tag{28}$$

The computational procedure used in this work is as follows. Firstly, pressure is imposed in the left and right boundary of the network. Subsequently, the pressure in each node is computed from the linear system resulting from the mass conservation in each node. For solving this system, we consider Dirichlet boundary conditions in the left and right boundaries and homogeneous Neumann boundary condition for the upper and lower boundary. The pressures in each node are used to compute the flux in each tube by means of equation (1). After this step, we proceed to solve the transport diffusion equation for the nutrients and we compute the concentration of nutrients in each node as well as the volume of biofilm in the tubes. The thickness of the biofilm and the radius of the void space available for water is updated and this process starts again at the next time step (See Figure 4).

4 Simulation Results

In this section, we show the effects of the biofilm growth on the hydrodynamics properties of the system.

Parameters for the second series simulation		
Name	Symbol	Value
Mean pore radius	R	12.2×10^{-6} $[m]$ [7]
Pore length	l	95×10^{-6} $[m]$
Global pressure gradient	ΔP	1.6 $[kPa/m]$
Viscosity of water	μ	0.001/60 $[Pa \cdot min]$
Density of water	ρ_w	1000 $[kg/m^3]$
Density of biofilm	ρ_{bf}	20 $[kg/m^3]$ [13]
Yield coefficient	Y	0.34 [2]
Half saturation constant for biofilm	E_{sb}	2×10^{-3} $[kg/m^3]$ [2]
Inlet reservoir concentration	C_{in}	1 $[kg/m^3]$
Initial biomass concentration	b_0	1×10^{-6} $[kg/m^3]$
Biofilm / bulk water viscosity ratio	β	10^7 [18]

Table 2

We present the results obtained for the biofilm growth factor $k_1 = 10^{-4}[1/s]$ and the detachment rate factor $k_2 = 10^{-6}[1/s]$. For this set of simulations we used a mesh with 100 x 60 elements and we consider a radius $R = 1.2 \times 10^{-5}[m]$ for all the tubes of the network. Additionally, only 4% of the tubes was seeded with the initial concentration of biofilm $b_0 = 1 \times 10^{-6}$ $[kg/m^3]$. The complete set of parameters for this set of simulations is listed in Table 2.

Subsequently, we study the evolution of the flux at the outlet of the domain of computation over time. We performed nine simulations where we kept all the parameters constant except the initial distribution of tubes seeded with biofilm. In Figure 5 the average of the normalized flux Q_n and its 95% confidence interval for the first set of simulations is presented,

$$Q_n = \frac{Q}{Q_0}, \tag{29}$$

where Q_0 is the initial flux in the network (i.e. without biofilm growth). We observe a decrease of the normalized flux due to the accumulation of biomass in the network. The development of biofilm attached to the walls of the pores leads to a reduction in the radius available for the water flow and consequently biofilm growth leads to a reduction of the normalized flux of the network.

We present the results obtained for the biofilm volume evolution in the network in Figure 6. Here, the average fraction of the volume of biofilm in the network, V_{pbf} and its 95% confidence interval is shown. The fraction of volume of biofilm in the network is

computed as follows,

$$V_{pbf} = \frac{\sum_{ij} V_{bf_{ij}}}{\sum_{ij} V_{ij}}, \tag{30}$$

in which $V_{bf_{ij}}$ is the volume of biofilm in the tube t_{ij} and V_{ij} is the volume of the tube t_{ij}. The sums are taken over all the tubes in the network. We observe that the volume of biofilm in the network increases monotonically. This holds during the period where the amount of biomass is still small, that is during the early stages of the injection. However, after some period the detachment prevails and then the volume of biofilm decreases. After 300 minutes, we observe that approximately 25% of the void space of the network is occupied by the volume of biofilm.

Since the biofilm blocks the pores, it is reasonable to assume that the normalized flux decreases with an increasing mass of biofilm. Furthermore, we postulate that the decrease of the normalized flux obeys a Power-Law with respect to the normalized flux itself. To this extent, we propose that the change in the normalized flux with respect to the fraction of volume of biofilm is described by the following equation,

$$\frac{dQ_n}{dV_{pbf}} = -\frac{c}{{Q_n}^{\alpha}} \tag{31}$$

in which Q_n is the normalized flux through the network, V_{pbf} is the partial volume of biofilm in the network, c is a positive constant and α is an exponent that can be positive or negative depending on the behavior of the biofilm growth in the network.

Since $Q_n > 0$ and $c > 0$, this implies that $\frac{dQ_n}{dV_{pbf}} < 0$ which means that as the amount of biofilm in the network increases, there is a reduction of the flux through the network due to the clogging of the pores in the network. Moreover, when α is positive, Q_n is close to one, the reduction of the flux due to biomass accumulation is slower than in the latest stages ($Q_n \sim 0$) in which the reduction of the flux is more significant. In this case, at early stages, the biofilm grows more uniformly through the network. However, at the latest stages, the inlet is plugged causing a dramatic reduction in the flux. If α is negative, then there is an exponential reduction of the flux due to biomass accumulation. Therefore, there is a preferential biofilm growth in the inlet of the network since early stages.

After solving equation (31) two parameters need to be determined: the constant c and the exponent α. These parameters are determined in order to fit this analytical function with the numerical data. In order to obtain the constant c, we consider the maximum value of V_{pbf} based on our numerical results. We define $\hat{V}_{pbf}$ as the maximum fraction of the volume of biofilm and $\hat{Q}_n$ as the flux at the maximum fraction of the volume of biofilm $Q_n(\hat{V}_{pbf}) = \hat{Q}_n$. Therefore, we can write the solution of equation (31) as,

$$Q_n = \left[1 + (\hat{Q}_n^{\alpha+1} - 1)\frac{V_{pbf}}{\hat{V}_{pbf}}\right]^{\frac{1}{\alpha+1}}, \tag{32}$$

in which Q_n is the normalized flux, $\hat{Q}$ is the flux at the maximum fraction of the volume of biofilm and $\hat{V}_{pbf}$ is the maximum fraction of the volume of biofilm. We used least square

Alpha parameter		
Growth coefficient k_1 $[1/s]$	Detachment rate k_2 $[1/s]$	α parameter
10^{-4}	10^{-6}	0.129

Table 3

fitting in order to obtain the value of the α exponent. In Table 3 we present the result obtained for an analytical fitting for $k_1 = 10^{-4}[1/s]$ and $k_2 = 10^{-6}[1/s]$.

Figure 7 shows the relation between the average normalized flux (with its 95% confidence interval) and the fraction of the volume of biofilm in the network. Furthermore, the analytical fit resulting from solving equation (31) is also shown in this figure. In Figure 8 the average normalized flux as a function of the porosity is shown for our numerical results with the 95% confidence interval. Additionally, in the same figure the analytical fit resulting from equation (31) is shown.

The next step is to make a comparison between our results, two cases of static biofilm growth and the Kozeny Carman relation. In the two cases of static biofilm growth, it is assumed that the nutrients are available in all the tubes in the network. Then an amount of biofilm is set in the network and the flux through the network is computed. In the first case, a uniform growth of biofilm in the network is assumed. In the second case, the number of tubes filled with biofilm was increased using a random distribution in each stage, from 1% of the tubes to 100% of the tubes. In the case of random biofilm growth, we perform 20 simulations and we obtain the average flux in the outlet of the network. In Figure 9 the average flux and its 95% confidence interval for the random biofilm growth are presented.

The porosity for our model is computed as follows,

$$\phi = \frac{V_{T_w}}{V_T}, \tag{33}$$

in which

$$V_{T_w} = \sum_{ij} V_{w_{ij}}, \tag{34}$$

is the total void space in the network. Furthermore,

$$V_T = 2RL_xL_y, \tag{35}$$

is an approximation of the total volume of the network. In this approximation, R is the radius of the tube, L_x and L_y is the length in the x and y directions respectively.

The Kozeny Carman equation relates the porosity ϕ and the permeability K and is given by,

$$K = C_k \frac{\phi^3}{(1-\phi)^2}, \tag{36}$$

in which C_k is a parameter related to the specific internal surface area.

On the other hand, the permeability is related to the flux by Darcy's Law,

$$K = QL\mu/\Delta PA, \tag{37}$$

where Q is the total flow through the outlet, ΔP is the pressure drop across the network, L the length of the network in the flux direction and A is the cross-sectional area at the outlet. Further, if the pressure drop, the cross-sectional area, the length of the network and the viscosity of the fluid are constant we have that,

$$\frac{K}{K_0} = \frac{Q}{Q_0}, \tag{38}$$

in which K_0 is the initial permeability.

Using equation (36) and equation (38) we have that,

$$\frac{Q}{Q_0} = \frac{(1-\phi_0)^2\phi^3}{\phi_0^3(1-\phi)^2}, \tag{39}$$

in which ϕ_0 is the initial porosity. In Figure 10 the numerical results and the analytical fit of the porosity ϕ versus the flux are shown. Additionally, the two cases of static biofilm growth and the Kozeny Carman relation are plotted in the same figure. We remove the confidence interval in this figure to ease the reading.

For high fluxes, the correspondence between the full model and Kozeny Carman is best. However as porosity decreases and the flux decreases, then the full model starts deviating the from other models. We observe that the average normalized flux Q_n computed with our model is lower than the normalized flux predicted by the Kozeny-Carman equation. This is explained by the fact that the biofilm growth is located preferentially in the inlet of the network due to the high concentration of nutrients, which causes a faster decrease in the flux through the network. The uniform biofilm growth has a similar behaviour as the Kozeny Carman equation though with a different rate. Finally, the random biofilm growth predicts less amount of biomass to plug the flux through the network in comparison to uniform biofilm growth and the Kozeny Carman equation.

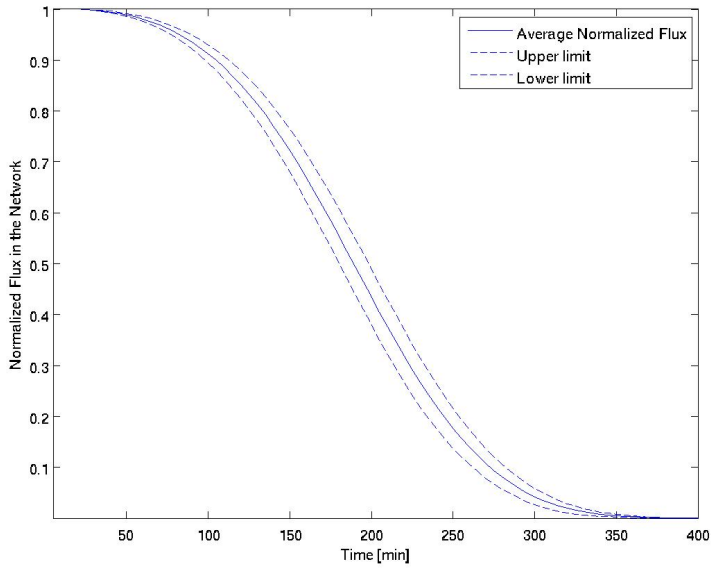

Figure 5: Average Normalized Flux and its confidence interval for $k_1 = 10^{-4}$, $k_2 = 10^{-6}$.

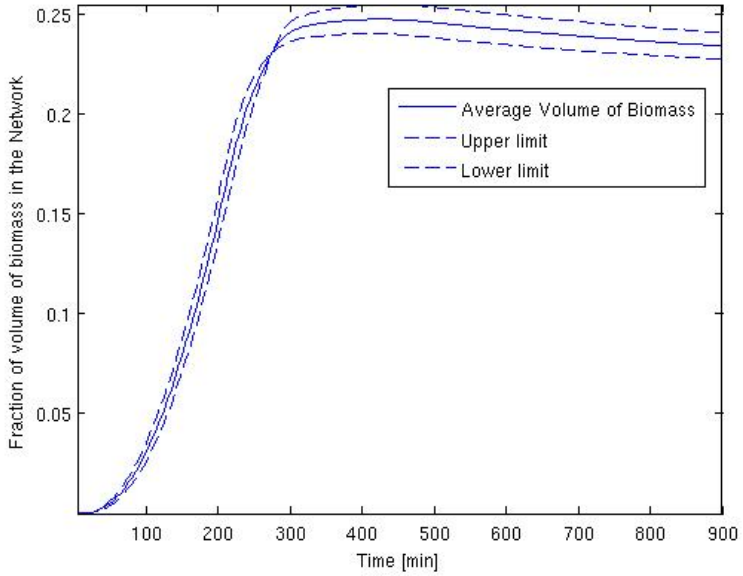

Figure 6: Average biomass in the Network for $k_1 = 10^{-4}$, $k_2 = 10^{-6}$.

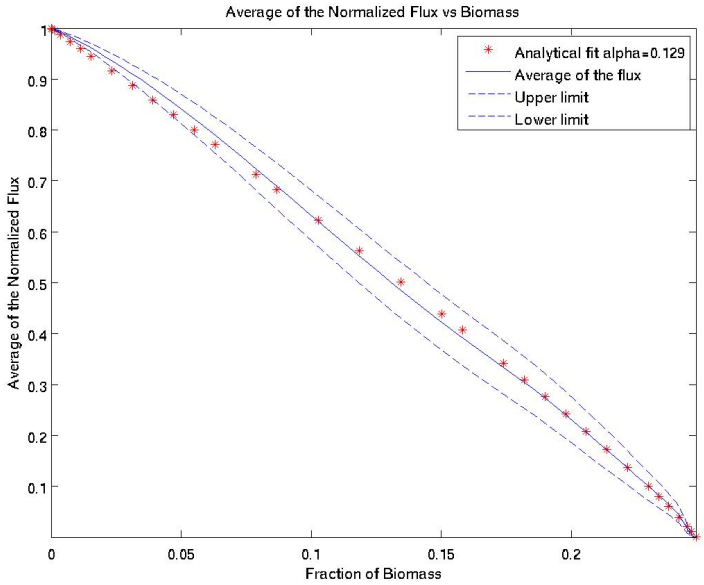

Figure 7: Average flux vs Biomass for $k_1 = 10^{-4}$, $k_2 = 10^{-6}$.

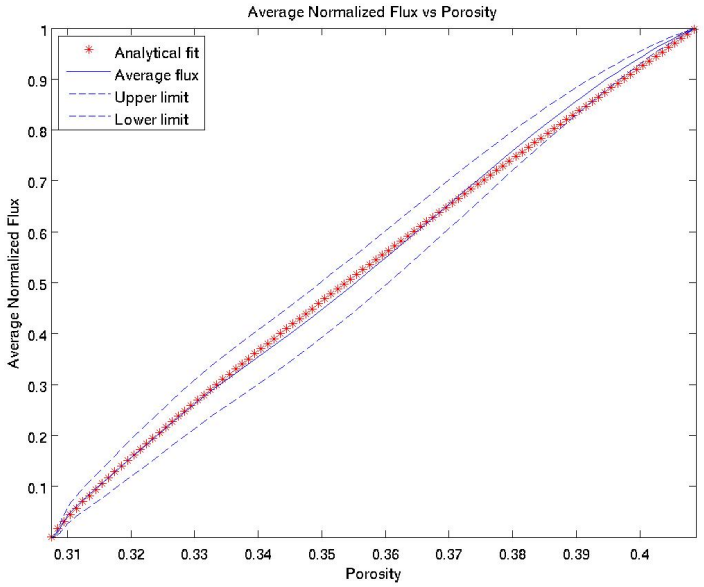

Figure 8: Average normalized Flux vs Porosity for $k_1 = 10^{-4}$, $k_2 = 10^{-6}$.

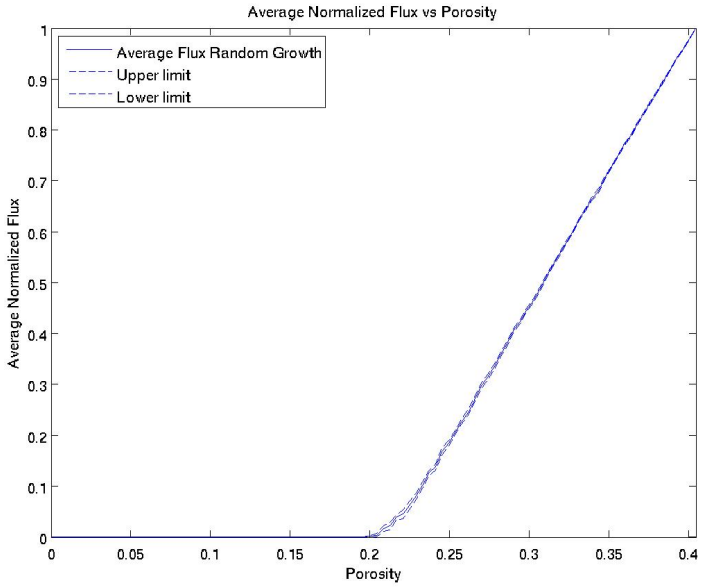

Figure 9: Average normalized Flux vs Porosity for random biofilm growth.

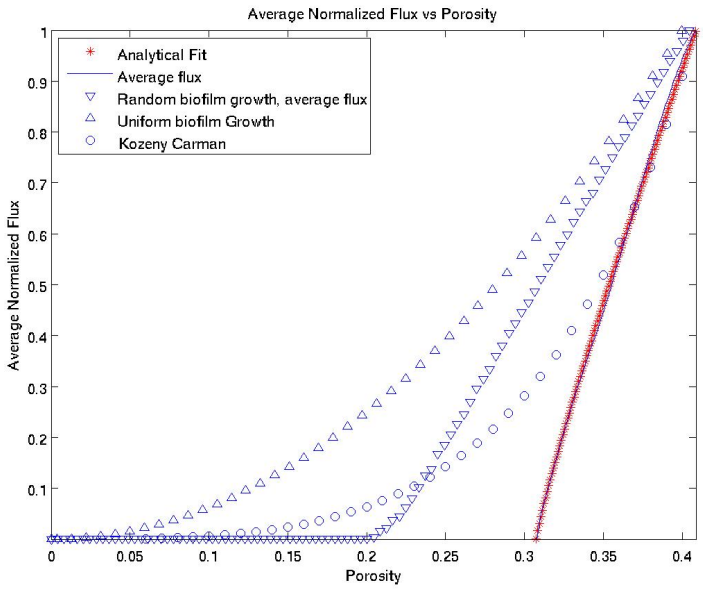

Figure 10: Average normalized Flux vs Porosity comparison

5 Discussion and Conclusions

In this work, we study biofilm growth in a porous medium and its effects on the porous medium characteristics such as porosity and permeability. We use a two-dimensional pore network model to represent the porous medium. The model incorporates the growth of biofilm when the nutrients get into contact with the biofilm. As we treat the biofilm as an impermeable layer, the nutrients will get into contact with the biofilm in the interfacial water-biofilm area. For this reason, we propose a new model in which the volumetric growth rate of biofilm is proportional to the interfacial water-biofilm area and where the biofilm growth is influenced by the concentration of nutrients via Monod Kinetics. This model allows the spreading of the biofilm through the whole network which is a phenomenon that has been observed experimentally. We studied the changes in the permeability and in the porosity caused by biofilm growth. Based on our numerical results we observed that the decrease of the permeability and porosity are determined for the clogging of the pores adjacent to the inlet. Additionally, we propose a phenomenological analytical relation between the flux and the amount of biofilm in the network. We performed a comparison between our results and the Kozeny-Carman relation. For a certain amount of biomass, our model predicts a larger reduction of the outward flux than one can predict using Kozeny Carman equation. The analytical relation between the volume of biomass and the permeability obtained in this work can be used for a future up-scaling technique to the real reservoir scale in oil reservoir simulations. To this extent we consider a 2D rectangular pore network model consisting of cylindrical tubes with the same radius, this assumption could be very simple to describe a real reservoir field. However, with our model we can observe the difference between a homogeneous growth which can be effectively described by a Kozeny Carman relation and a preferential growth of biofilm, like in this particular case, the biofilm growth near the inlet of the network. Interesting further research could be the study of the effects of biofilm growth in porosity and permeability in more complex topologies in 2D and 3D. Finally, it is important to mention that this type of model can be extended to model different kinds of problems such as atherosclerosis which is a disease of arteries by fatty deposition.

References

[1] Armstrong, R., and Wildenschild, D. Investigating the pore-scale mechanisms of microbial enhanced oil recovery. *Journal of Petroleum Science and Engineering 94-95* (2012), 155–164.

[2] Bakke, R., Trulear, M., Robinson, J., and Characklis, W. Activity of pseudomonas aeruginosa in biofilms: steady state. *Biotechnology and bioengineering 26*, 12 (1984), 1418–1424.

[3] Behlulgil, K., Mehmetoglu, T., and Donmez, S. Application of microbial enhanced oil recovery technique to a turkish heavy oil. *Applied microbiology and biotechnology 36*, 6 (1992), 833–835.

[4] Brown, L. R. Microbial enhanced oil recovery (meor). *Current opinion in Microbiology 13*, 3 (2010), 316–320.

[5] Chen-Charpentier, B. Numerical simulation of biofilm growth in porous media. *Journal of computational and applied mathematics. 103* (1999), 55–66.

[6] Costa, A. Permeability-porosity relationship: A reexamination of the kozeny-carman equation based on a fractal pore-space geometry assumption. *Geophysical research letters 33*, 2 (2006).

[7] Ezeuko, C., Sen, A., A., G., and Gates, I. Pore-network modelling of biofilm evolution in porous media. *Biotechnology and Bioengineering 108* (2011), 2413–2423.

[8] Graf von der Schulenburg, D., Pintelon, T., Picioreanu, C., van Loosdrecht, M., and Johns, M. Three-dimensional simulations of biofilm growth in porous media. *AIChe Journal 55* (2008), 494–504.

[9] Lazar, I., Petrisor, I., and Yen, T. Microbial enhanced oil recovery (meor). *Petroleum Science and Technology 25*, 11 (2007), 1353–1366.

[10] Li, Q., Kang, C., Wang, H., Liu, C., and Zhang, C. Application of microbial enhanced oil recovery technique to daqing oilfield. *Biochemical Engineering Journal 11*, 2 (2002), 197–199.

[11] Picioreanu, C., Kreft, J.-U., and van Loosdrecht, M. C. Particle-based multidimensional multispecies biofilm model. *Applied and environmental microbiology 70*, 5 (2004), 3024–3040.

[12] Pintelon, T., Graf von der Schulenburg, D., and Johns, M. Towards optimum permeability reduction in porous media using biofilm growth simulations. *Biotechnology and Bioengineering 103* (2009), 767–779.

[13] Ro, K. S., and Neethling, J. Biofilm density for biological fluidized beds. *Research journal of the water pollution control federation* (1991), 815–818.

[14] Samsó, R., García, J., Molle, P., and Forquet, N. Modelling bioclogging in variably saturated porous media and the interactions between surface/subsurface flows: Application to constructed wetlands. *Journal of environmental management 165* (2016), 271–279.

[15] Sen, R. Biotechnology in petroleum recovery: the microbial eor. *Progress in Energy and Combustion Science 34*, 6 (2008), 714–724.

[16] Suchomel, B., Chen, B., and Allen, M. Macroscale properties of porous media from a network model of biofilm processes. *Transport in porous media. 31* (1998), 39–66.

[17] Thullner, M. Comparison of bioclogging effects in saturated porous media within one-and two-dimensional flow systems. *Ecological Engineering 36*, 2 (2010), 176–196.

[18] Thullner, M., and Baveye, P. Computational pore network modeling of the influence of biofilm permeability on bioclogging in porous media. *Biotechnology and Bioengineering 99*, 6 (2008), 1337–1351.

[19] Thullner, M., Zeyer, J., and Kinzelbach, W. Influence of microbial growth on hydraulic properties of pore networks. *Transport in porous media. 49* (2002), 99–122.

[20] Van Wijngaarden, W., Vermolen, F., Van Meurs, G., and Vuik, C. A mathematical model and analytical solution for the fixation of bacteria in biogrout. *Transport in porous media 92*, 3 (2012), 847–866.

[21] Xu, P., and Yu, B. Developing a new form of permeability and kozeny–carman constant for homogeneous porous media by means of fractal geometry. *Advances in water resources 31*, 1 (2008), 74–81.

[22] Yakimov, M. M., Amro, M. M., Bock, M., Boseker, K., Fredrickson, H. L., Kessel, D. G., and Timmis, K. N. The potential of bacillus licheniformis strains for in situ enhanced oil recovery. *Journal of Petroleum Science and Engineering 18*, 1 (1997), 147–160.